DOI 10.5012/bkcs.2011.32.6.1865

Characteristics of a Metal-loaded SnO_2/WO_3 Thick Film Gas Sensor for Detecting Acetaldehyde Gas

Jae-Mok Jun, Young-Ho Park,† and Chang-Seop Lee*

*Department of Chemistry, Keimyung University, Daegu 704-701, Korea. *E-mail: surfkm@kmu.ac.kr*
†Department of Pharmaceutical Engineering, International University of Korea, Gyeongnam 660-759 Korea
Received March 16, 2011, Accepted April 6, 2011

This study investigates the sensitivity of a gas sensor to volatile organic compounds (VOCs) at various operating temperatures and catalysts. Nano-sized powdered WO_3 prepared by sol-gel and chemical precipitation methods was mixed with various metal oxides. Next, transition metals (Pt, Ru, Pd, and In) were doped on the surface of the mixture. Metal-WO_3 thick films were prepared using the screen-printing method. The physical and chemical properties of the films were studied by SEM/EDS, XRD, and BET techniques. The measured sensitivity to VOCs is defined as the ratio (R_a/R_g) of resistance (R_{air}) of WO_3 film in the air to resistance (R_{gas}) of WO_3 film in a VOCs test gas. The sensitivity and selectivity of the films were tested with various VOCs such as acetaldehyde, formaldehyde, methyl alcohol, and BTEX. The thick WO_3 film containing 1 wt % of Ru and 5 wt % of SnO_2 showed the best sensitivity and selectivity to acetaldehyde gas at an operating temperature of 300 ºC.

Key Words : WO_3 gas sensor, Sol-gel, VOCs, Acetaldehyde, Thick film, Screen-printing

Introduction

Industrial development and increases in population and transportation have led to the advent of various environmental problems such as photochemical smog, the greenhouse effect, acid rain, and a decrease of the ozone layer in the stratosphere. In particular, a significant amount of pollutants harmful to the health and reproduction of humans, animals, and plants can be found in the planet's air, water, and soil. In this regard, volatile organic compounds (VOCs) are of interest. VOCs are substances that can easily be vaporized due to their high vapor pressure and can induce photochemical reactions when combined with nitrogen oxide in the air. As such, these VOCs cause photochemical smog by generating photochemical substances such as ozone and PAN. Long-term human exposure to VOCs can lead to serious problems including leukemia, central nervous system disorders, and reproductive problems. In terms of VOCs, acetaldehyde and formaldehyde have been regarded as two of the most widely air-disseminated carbonyl compounds. Aldehydes, which are generated by combustion and oxidization, are related to the photochemical reactions that produce ozone, increase global warming, and destroy the ozone layer in the stratosphere. Aldehydes usually exist as a gas form at room temperature and can remain in the air for a long time.

Acetaldehyde is the main source of toxic materials generated in new houses and can appear in the air both indoors and outdoors. Humans exposed to aldehydes risk a serious toxic reaction caused by the stimulation of respiratory organs such as the throat, nose, and bronchus. More serious risks include the creation of an anesthesia effect in the central nervous system, and, in excessive cases, extreme physical reaction such as paralysis, respiratory disorders, and even the onset of a comatose state.[1,2] Therefore, for both environmental and health reasons, it is very important to detect the presence of aldehydes.

The study of semiconductor gas sensors to detect gas was first conducted by Seiyama *et al*.,[3] and Taguchi *et al*..[4] Gas detection devices based on the effect of gas absorption-desorption on the surface of semiconductor oxides (SnO_2,[5] TiO_2,[6] and ZnO[3]) have been widely investigated, and studies involving WO_3,[7] Fe_2O_3,[8] and In_2O_3 [9] have also been reported. In the case of WO_3, the first study was conducted by Shaver,[10] where he revealed that the electrical conductance of WO_3 thin film changed when it came into contact with low concentrations of H_2 gas. Building upon Shaver's study, other researchers were able to manufacture thick film-type gas sensors to which WO_3, metal catalysts, and metal oxides were added. Gas detection and selectivity at low concentration ranges can be improved by adding metal catalysts such as Pd, Pt, and Ru. The addition of metal catalysts has been known to improve sensitivity characteristics by increasing stability and restraining particle growth. Since WO_3 is one of the most interesting and most researched gas sensor materials, a number of different types of sensors have recently been demonstrated including resistive,[20] optical,[21] and capacitive[22] devices for various gas analytes such as NOx,[23] NH_3,[24] CO,[25] H_2,[26] and H_2S.[27]

In this study, WO_3 as a main gas-sensing element was synthesized using a sol-gel process. Thereafter, a metal oxide of SnO_2 was added in order to stabilize the electrical characteristics. To enhance the selectivity and sensitivity of the gas sensor to detect gases, Pd, Pt, In, and Ru were added at the given weight ratios of these metal catalysts. The WO_3 thick film was manufactured based on the silk screen pro-

cess, which is not only economical but also enables mass production. We studied the optimal conditions of the gas sensor to detect acetaldehyde through the analysis of the characteristics of gas detection based on the experimental parameters of thermal treatment, the presence of metal oxides, and the amounts of metal catalysts added.

Experimental Section

Manufacturing of a Sensing Material for a Gas Sensor. In this study we synthesized WO_3 by a sol-gel process and used it as a sensing material to detect acetaldehyde. Figure 1 shows the synthesis sequence of nano-sized WO_3 powder. After dissolving 0.01 mol of WCl_6 in 0.1 L of ethyl alcohol (Aldrich) by stirring the solution for 36 hours at 70 °C, a homogenized sol of $W(OC_2H_5)_6$ was obtained. The gel powder of $W(OH)_6$ was extracted by titrating the solution of NH_4OH into the sol of $W(OC_2H_5)_6$ at pH lower than 5. For cleansing procedures, NH_4NO_3 solution, distilled water, and ethanol were used to remove the residual chlorine ions (Cl^-). The presence of residual chlorine ions (Cl^-) was verified by using $AgNO_3$ solution to test for the occurrence of a silver mirror reaction. After drying the cleansed precipitate for 12 hours at 100 °C and finishing the calcination process, the WO_3 nano powder was obtained.[11,12] Furthermore, in order to stabilize the electrical characteristics of the sensing material, we dissolved SnO_2 in distilled water at various composition ratios and then added it to the WO_3 while stirring the solution with a magnetic stirrer.

To enhance the essential functions of sensitivity and selectivity of the gas sensor, metal catalysts were added using the impregnation method shown in Figure 1.[13-15] In terms of the impregnation method, the transition metals of Pd, Pt, Ru, and In were weighed to give weight ratios of 1-5 wt % and then placed in a beaker. Next, 1 mL of hydrochloric acid (HCl) and distilled water were added to completely dissolve the metal catalysts. After having impregnated the metal catalysts by adding WO_3 powder or SnO_2/WO_3 powder to a homogenous solution, we obtained WO_3 powder or SnO_2/WO_3 powder containing metal catalysts by gradually heating and stirring the impregnated solution with a magnetic stirrer. After we dried the solution for 12 hours at 100 °C and calcinated it for 2 hours at 500 °C, we obtained the powder that was then crushed to produce a sensing material.

Fabrication and Structure of the Thick Film Gas Sensor. A commercial-use Pt electrode (0.5 mm) with a Ni-Cr built-in heater was used on the surface of alumina (Al_2O_3) substrate (13 mm × 8 mm × 0.67 mm). A complete cleaning process using acetone and a thermal treatment at 300 °C was done in order to remove the dirt from the surface of the substrate before the thick film was doped. Once these procedures had been completed, a 20 μm-thick sensing-material paste was coated on using the screen printing method. The thick film device formed through the above procedures was then dried for 24 hours at room temperature. Thereafter, the temperature was increased by 5 °C/10 min and the device was then dried once again in a convective drier for 12 hours

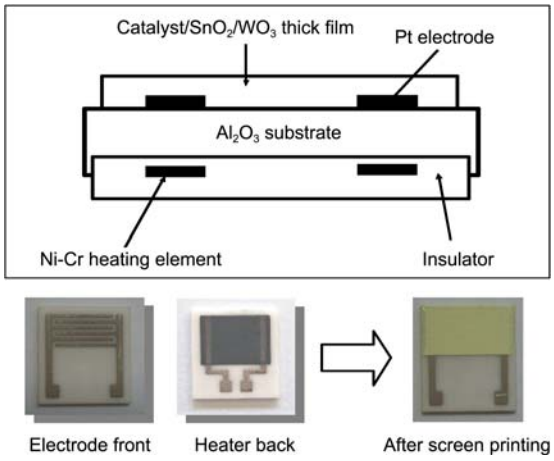

Figure 2. Schematic view of fabricated thick film sensors.

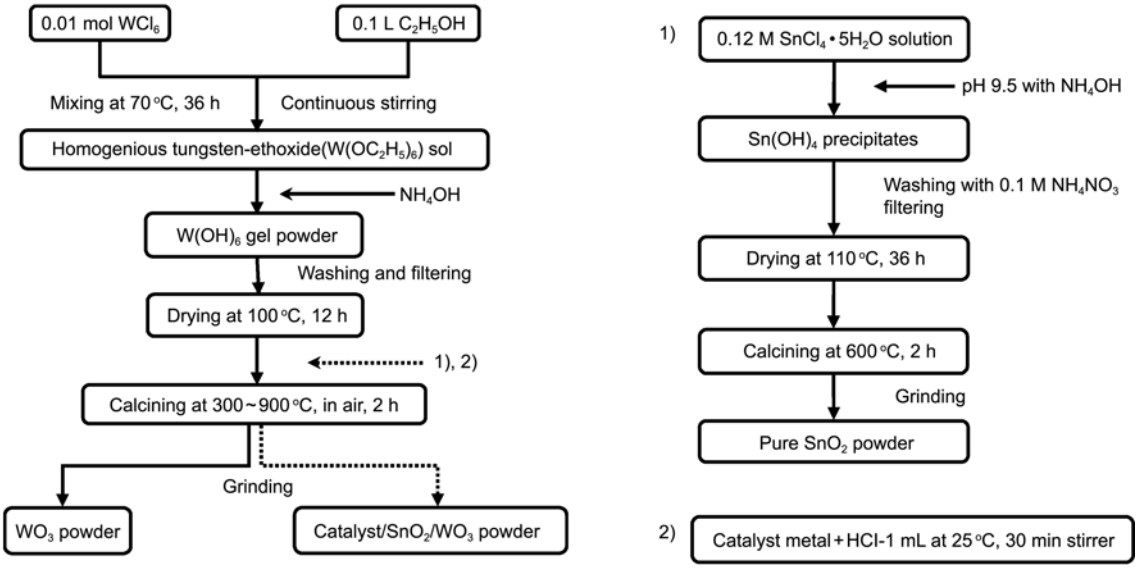

Figure 1. Synthesis sequence for sensor material.

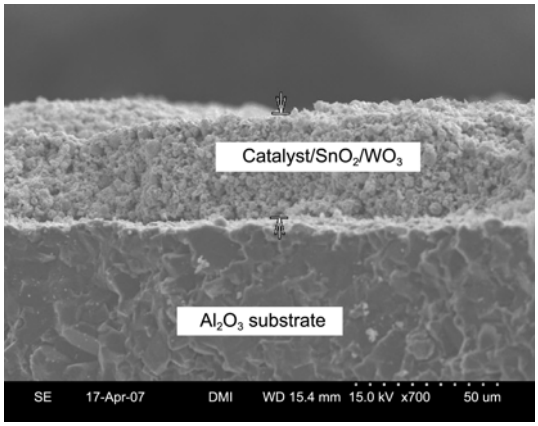

Figure 3. Cross-sectional view of thick film.

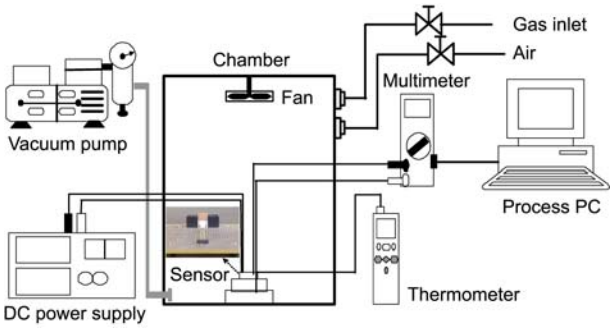

Figure 4. Apparatus used for gas-sensing experiments.

at 110 °C before undergoing a one-hour thermal treatment at 500 °C. Figure 2 shows the configuration of the thick film sensor and an image after the thick film was doped onto the substrate.[16]

Figure 3 shows an SEM image taken after the thick film was homogeneously doped on the surface of the alumina substrate.

Analysis of Sensitivity Characteristics. Fixing the gas sensor at a distance of 50 mm from the bottom of a 10 L (250 mm × 200 mm × 200 mm) container, we measured the sensitivity of the gas sensor in the temperature range of 200-400 °C. In order to remove the electrons in the device, a stabilization procedure was carried out for 12 hours at the same temperature as the one used for measurements. After the sensor gas was introduced into the container with the fan on, the resistance was measured with an electrometer after the equilibrium concentration was reached. The sensitivity of the sensor was defined as the ratio of electrical resistance (R_g) after the injection of sensor gas to the electrical resistance (R_a) in the air, or R_a/R_g. Figure 4 displays the experimental model used to measure gases in this study.

Results and Discussion

Analysis of Sensing Materials Used for the Gas Sensor. In this study we manufactured sensing materials for a gas-detecting sensor using various composition ratios of WO_3 powder employed as a main sensing element to metal oxide (SnO_2) and metal catalysts. XRD, SEM/EDS, and BET

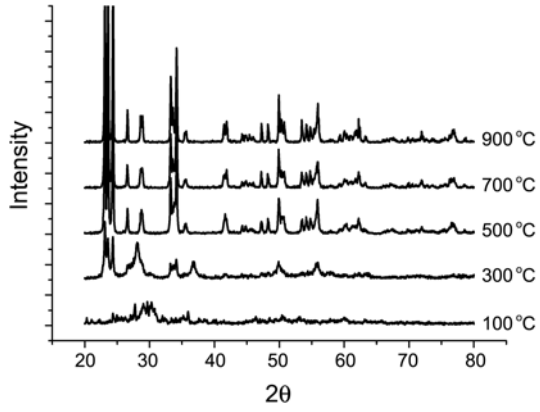

Figure 5. X-ray diffraction pattern of WO_3 powder.

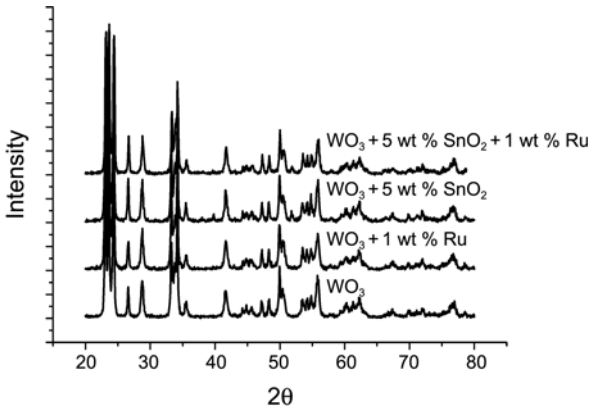

Figure 6. X-ray diffraction patterns of catalyst/SnO_2/WO_3.

equipment were used to analyze the crystallization, phase, and surface state, elemental analysis, and ratios of surface areas. Figure 5 shows the XRD patterns of WO_3 at different calcination temperatures, and Figure 6 shows the XRD patterns when metal oxide (SnO_2) and metal catalysts were added to WO_3. As we can see from Figure 5, the peak intensity of WO_3, which is an indication of crystallization, increases as the calcination temperature gets higher. This means that the crystallization increases with raising the calcination temperature. Based on the comparison of the data we obtained in this study with those of JCPDS, which were employed as reference data, we found that our experimental results are consistent with those related to orthorhombic structure, which is one of three structures of WO_3[17]. Figure 6 demonstrates that as metal catalysts and metal oxides were added, new peaks started to show up at certain 2θ values.

Figure 7 exhibits SEM images of WO_3 thick film at various calcination temperatures. These SEM images show that the particle size of WO_3 thick film increases as the calcination temperature rises.

Figure 8 represents SEM images and EDS results of each sensing material composed of WO_3 containing metal oxides and metal catalysts. Figure 8(a) shows SEM images and EDS results for sensing material of WO_3 only. Figure 8(b) shows SEM images and EDS results for sensing material of 5 wt % SnO_2/WO_3. Figure 8(c) shows SEM images and EDS results for sensing material of 1 wt % Ru/WO_3. Figure 8(d)

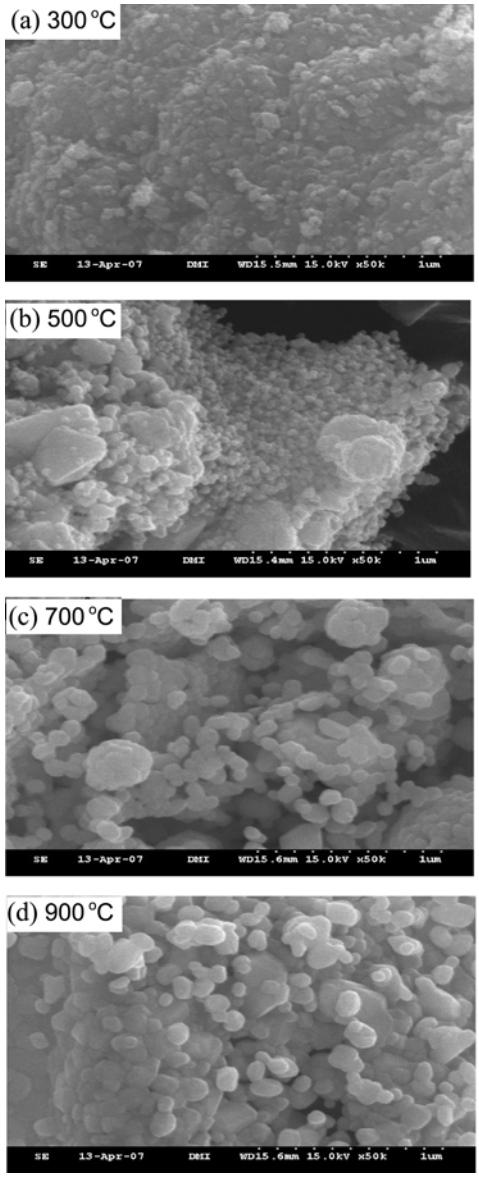

Figure 7. SEM image of WO_3 powders calcined for 2 h at 300 °C (a), 500 °C (b), 700 °C (c), 900 °C (d).

shows SEM image and EDS results for sensing material of 1 wt % Ru/5 wt % SnO_2/WO_3. The SEM images clearly expose the surface of each sensing material. The EDS results demonstrate the emergence of new peaks of component element in the case of each sensing material.

Figure 9 shows the results of measurements of pore distribution after SnO_2 was added. The sensing material containing 5 wt % of SnO_2 showed more uniform pore distribution than other sensing materials. Table 1 exhibits the specific surface area of individual sensing materials based on the amount of SnO_2 added. This table reveals that the sensing material to which 5 wt % of SnO_2 was added, which as mentioned above demonstrated relatively uniform pore distribution, also exhibited the biggest surface area of 14.83 m^2/g. This can be explained in that the addition of SnO_2 to WO_3 caused a restraint in particle growth, which in turn caused an increase in surface area and an improvement in sensitivity.

Temperature Effects on Sensing Materials. Figure 10 exhibits the sensitivity of the WO_3 thick film sensor to acetaldehyde gas of 100 ppm concentration at various operation temperatures and calcination temperatures. To this end, WO_3 calcinated at 500 °C showed the highest sensitivity at 350 °C. Figure 11 exhibits the sensitivity of the sensor to acetaldehyde gas of 100 ppm concentration at different operation temperatures when SnO_2 and metal catalysts were added. While the sensitivity reached the highest at 350 °C in the case of WO_3 alone, it reached its peak at 300 °C when SnO_2 and Ru were added to WO_3. This can be understood as the result of the fact that, depending on the amount of SnO_2 and the type of metal catalyst added, the activation energy underwent a rapid change at a given temperature. Thereafter, the experiments were conducted at a fixed operation temperature of 300 °C. It was found that the sensitivity became worse at temperatures higher than 300 °C. According to a report by Mcaleer *et al*.,[18] as temperature goes up, the surface of the sensor becomes more activated, which leads to the enhancement in sensitivity. However, once critical temperature is reached, the desorption of the adsorption species of reductive gas, as well as the re-adsorption of the adsorption species in the air, occurs rapidly, and the gas for detection reacts at the surface of the electrode. This effectively prevents the sensor gas from infiltrating the electrode, thereby causing a lowering of the sensitivity of the sensor.

Gas Sensing Characteristics of WO_3 Thick Film at Various Weight Ratios of SnO_2. Figure 12 exhibits the results of the sensitivity characteristics of the WO_3 thick film sensor to detect acetaldehyde gas at various weight ratios of SnO_2. Such a study was conducted in order to improve the stability of the gas sensor, an attribute considered to be essential. As we can see from Figure 12, the sensitivity increased as the concentration of SnO_2 increased, and it reached its maximum at 5 wt % of SnO_2 addition. Since this sensing material shows the best sensitivity in our work and it is consistent in that it shows the best pore distribution and ratio of surface area in earlier work, we reached the conclusion that the uniform pore distribution and other physical properties produced by an increase in the specific surface area affect the sensitivity of the gas sensor.

Gas Sensing Characteristics Improved by Adding Various Metal Catalysts. To enhance the sensitivity and selectivity of the gas sensor to acetaldehyde gas, metal catalysts were added to the sensing material. When a metal catalyst is mixed to a metal oxide, there is an increase in the adsorption species due to the activation of electrons, which affect the adsorption-desorption process and result in an increase in electrical conductivity. To elevate the effect of this catalyst reaction, the area in which the metal catalysts come into contact with the sensor gas should be increased. Such a move has been found to greatly influence sensitivity, selectivity, and operation temperature in terms of gas-sensing.[19]

Figure 13 exhibits the sensitivity characteristics of sensing materials to acetaldehyde gas by varying the metal catalysts. Here, we added various metal catalysts to 5 wt % SnO_2/WO_3,

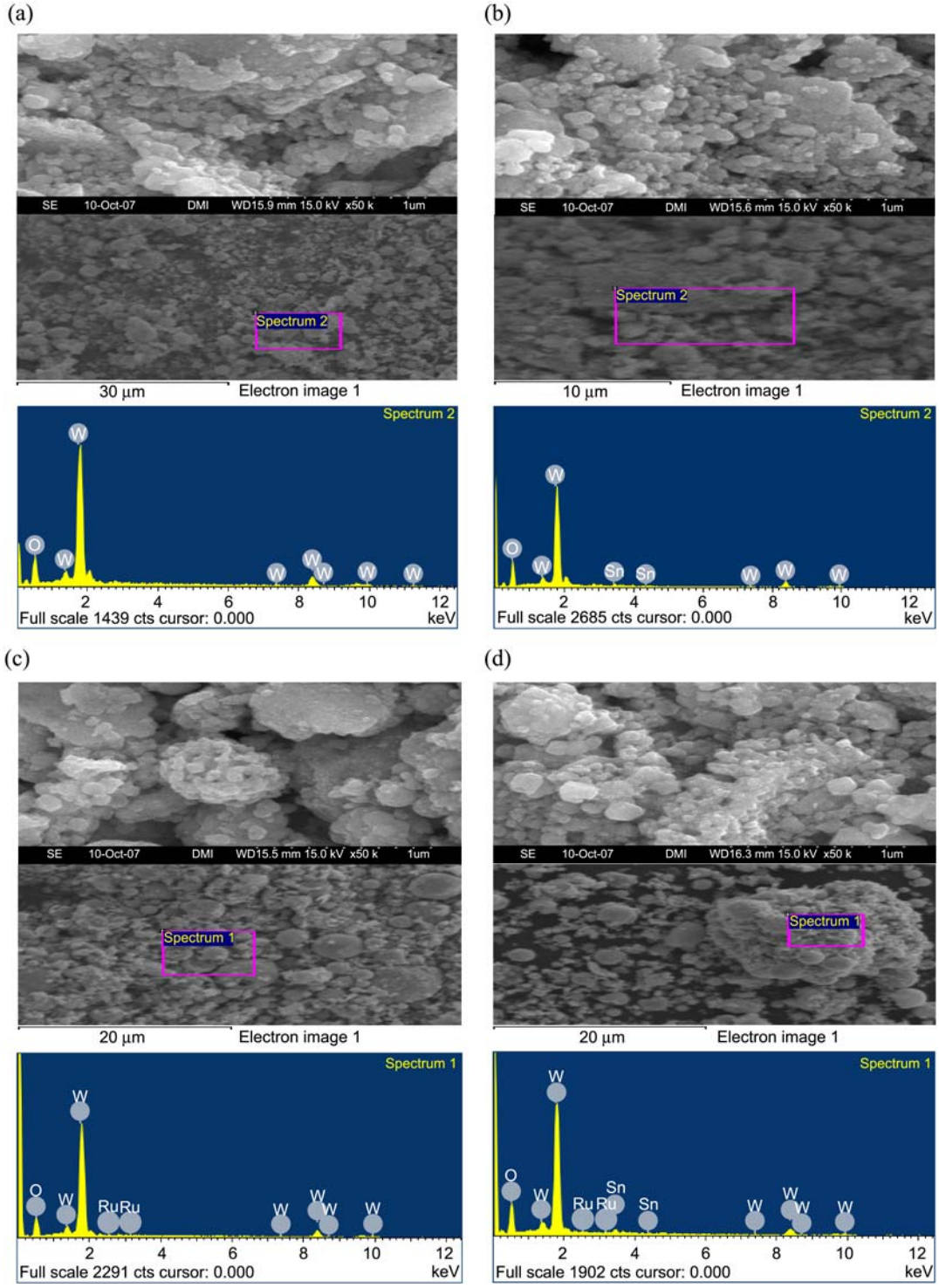

Figure 8. SEM image and EDS results of gas sensing material, Upper: SEM (× 50 K), middle: SEM (5 K), below: EDS (× 5 K).

which was used as a basic sensing material. As we can see from Figure 13, the sensing material containing 1 wt % of Ru shows higher sensitivity than cases of other catalysts. This means that 5 wt % SnO_2/WO_3 with a metal catalyst of 1 wt % Ru exhibits superior selectivity by oxidizing acetaldehyde gas at a faster speed than other sensing materials. The reason we used 1 wt % concentration is that it gave the best sensitivity; that is, in the range of 0-1 wt %, the sensitivity is increased with increasing the Ru concentration. On the other hand, if the concentration exceeds 1 wt %, the sensitivity drops. In the sensor material more than 1 wt % of Ru was added. The Ru particles conglomerated, so they were not able to spread homogenously on the surface of the thick film. This caused a decrease in specific surface area and also the sensitivity of the sensor.

Gas Sensing Characteristics at Various Film Thick-

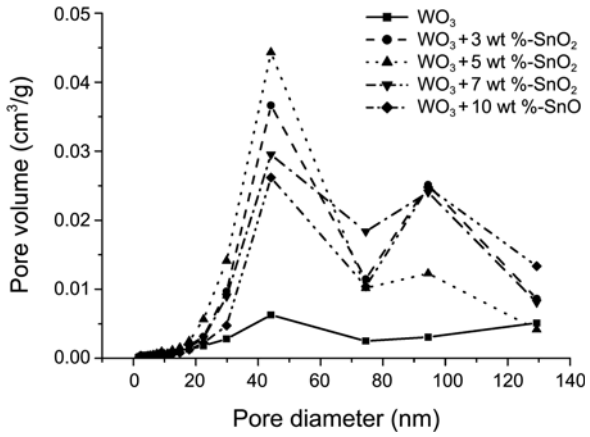

Figure 9. BJH pore size distribution of various amounts of SnO_2.

Table 1. Surface area (m^2/g), pore diameter (nm), pore volume (cm^3/g) of 0-10 wt % SnO_2/WO_3

Samples	BET surface area (m^2/g)	Pore diameter (nm)	Total pore volume (cm^3/g)
WO_3	6.6713	11.72	0.029713
$WO_3 + SnO_2$ (3 wt %)	13.4527	18.37	0.103673
$WO_3 + SnO_2$ (5 wt %)	14.8296	20.74	0.101604
$WO_3 + SnO_2$ (7 wt %)	12.5545	17.08	0.100055
$WO_3 + SnO_2$ (10 wt %)	10.8391	16.20	0.088917

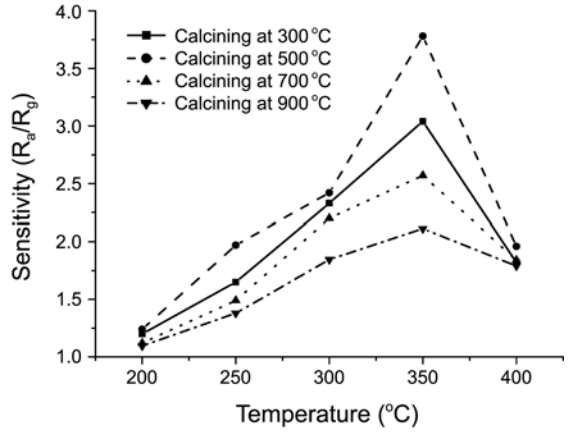

Figure 10. Sensitivity of WO_3 thick films with various calcination temperatures for acetaldehyde gas (100 ppm) with different operating temperatures.

nesses. Figure 14 exhibits the sensitivity characteristics to acetaldehyde gas of various thicknesses of film doped on the substrate. This test revealed that the sensitivity decreased as the thickness of film increased. The best sensitivity was recorded at a film thickness of 20 μm.

Gas Sensing Characteristics at Low Concentration Range. Figure 15 represents the sensitivity characteristics to acetaldehyde gas at a concentration range of less than 10 ppm using the sensing material to show the best sensitivity in this study. As is displayed, the sensitivity showed an almost linear increase with concentration even at low concentration

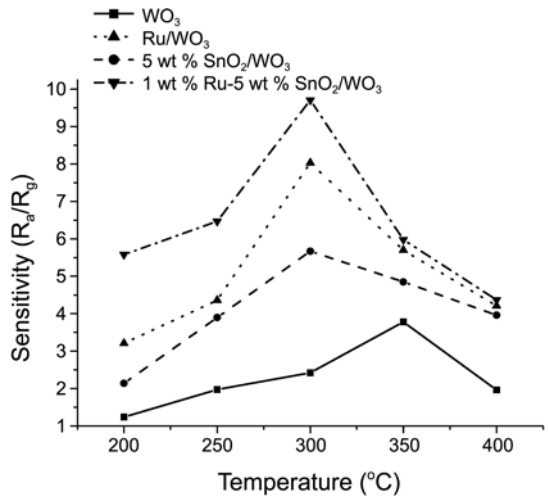

Figure 11. Sensitivity of gas sensor for acetaldehyde gas (100 ppm) at various temperatures.

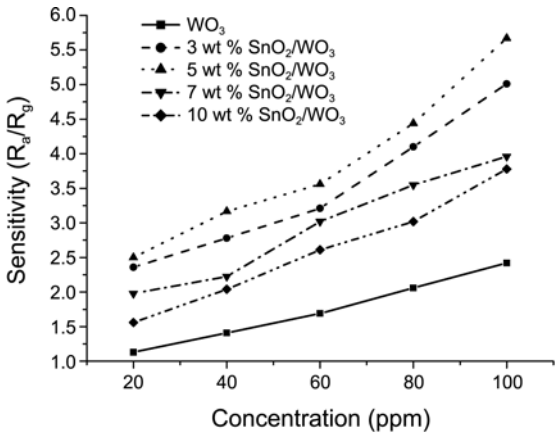

Figure 12. Sensitivity with amount of metal oxide to various concentration of acetaldehyde gas at 300 °C.

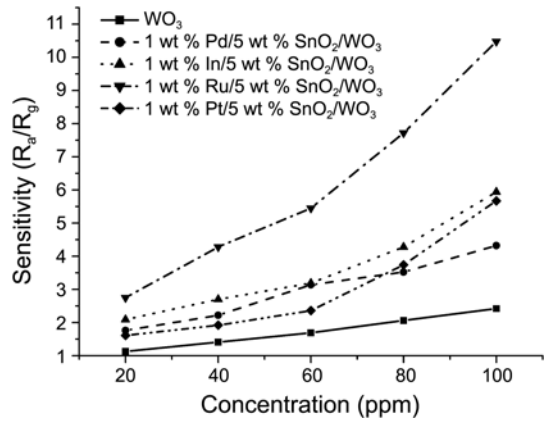

Figure 13. Sensitivity with catalyst/5 wt % SnO_2/WO_3 to various concentration of acetaldehyde gas at 300 °C.

ranges. In the image in the box, we can see a relatively linear growth in sensitivity in the wider concentration range (1-1000 ppm) of acetaldehyde when gas is applied.

Selectivity and Response-Recovery Characteristics of Sensing Materials with Various Gases. Figure 16 exhibits

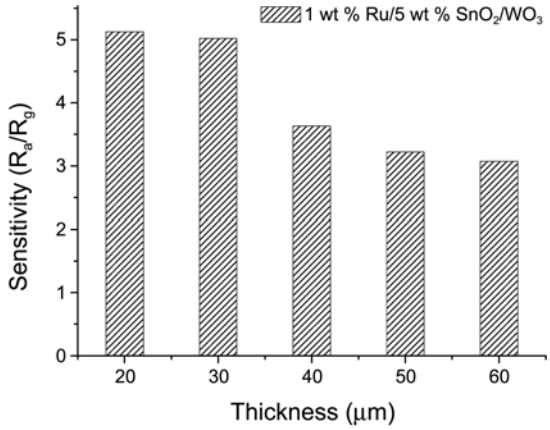

Figure 14. Sensitivity of gas sensor with 1 wt % Ru/5 wt % SnO_2/WO_3 thick films to acetaldehyde gas (50 ppm) at 300 °C.

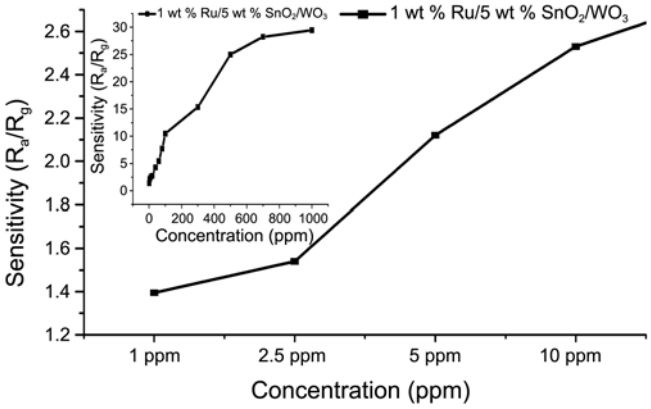

Figure 15. Sensitivity with 1 wt % Ru/5 wt % SnO_2/WO_3 from 1 ppm to 100 ppm of acetaldehyde gas at 300 °C (Inset: Sensitivity from 1 ppm to 1000 ppm).

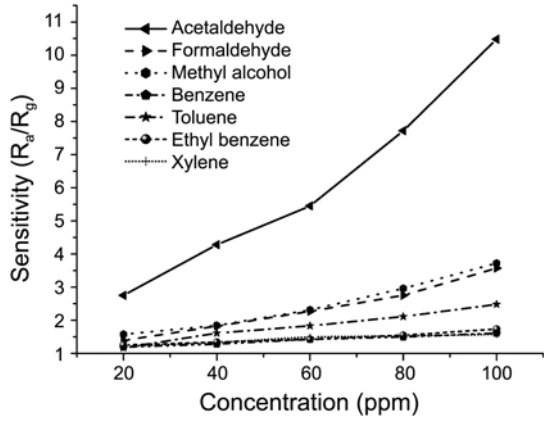

Figure 16. Sensitivity with 1 wt % Ru/5 wt % SnO_2/WO_3 to various gases (100 ppm) at 300 °C.

the results of the selectivity study of the sensing materials giving the best sensitivity to acetaldehyde gas to various VOC gases. The measurement of a sensitivity of 1 wt % Ru/5 wt % SnO_2/WO_3 gas sensor, which was found to give the highest sensitivity to acetaldehyde gas as well as to various gases within a concentration range of 100 ppm, revealed that

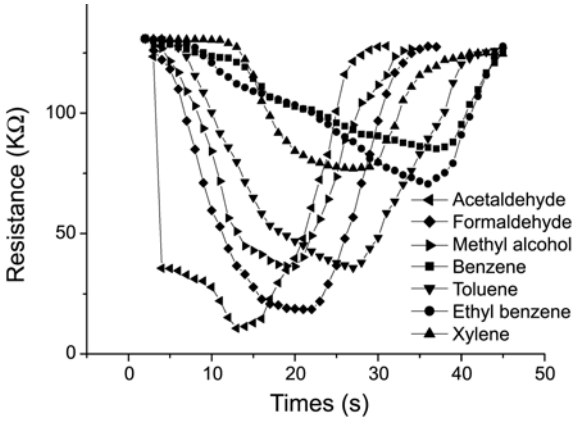

Figure 17. Response-Recovery characteristics of 1 wt % SnO_2/WO_3 to various gases (100 ppm).

its sensitivity toward acetaldehyde gas was much higher than its sensitivity to other gases. It can be understood that the sensing material of 1 wt % Ru/5 wt % SnO_2/WO_3 is better suited for decomposing acetaldehyde gas and activating a reaction therein than for other VOC gases.

Figure 17 exhibits the response-recovery characteristics to acetaldehyde gas and other VOC gases. In order to speed up the experiment process, the response-recovery characteristics were calculated based on forced exhausts. As we can see from the images in Figure 17, the response-recovery characteristics of the gas sensor to acetaldehyde gas were also more developed than in the case of other VOC gases.

Conclusions

In this study we manufactured a thick film gas sensor to detect acetaldehyde gas that featured WO_3 as its basic sensing material, and to which SnO_2 and various metal catalysts were added. Thereafter, we investigated the sensitivity characteristics of the gas sensor to acetaldehyde gas: (1) at various amounts of SnO_2 and with various types and amounts of metal catalysts; (2) at various calcination and operation temperatures; (3) by thickness of film; and (4) along with the response-recovery characteristics, to various other gases.

The gas sensor developed in this study used the electrical resistance created by VOCs absorption gas. The sensitivity characteristics of this thick film gas sensor, in which SnO_2 and metal catalysts had been added to the WO_3, exhibited a tendency to depend on factors such as the calcination and operation temperatures of WO_3, the type and concentration range of SnO_2 and metal catalysts, and the binder type and thickness of the film.

The ideal conditions for the sensing material in terms of detecting acetaldehyde gas were found to be a calcination temperature of 500 °C, an operation temperature of 300 °C, a film thickness of 20 μm, and the use of ethylene glycol as a binder. From a structural standpoint, the best sensitivity, selectivity, and response-recovery characteristics were obtained when 1 wt % Ru/5 wt % SnO_2 was added to WO_3 sensing

material.

The WO_3 thick film gas sensor developed in this study demonstrated high sensitivity to VOC gases at a low concentration range, and it exhibited an especially high selectivity toward acetaldehyde gas. To this end, it is expected that the gas sensor developed in this study could be used to detect gases that have been regarded as a root cause of environmental pollution.

References

1. Noordally, E.; Richmond, J.; Tabir, S. F. *Catalyst Today* **1993**, *17*, 359.
2. Hodgson, A. T.; Faulkner, D.; Sullivan, D. P.; Dibartolomeo, M. L.; Russel, D. L.; Fisk, W. J. *Atmospheric Environment* **2003**, *37*, 5517.
3. Seiyama, T.; Kata, A.; Fukiishi, K.; Nagatini, M. *Anal. Chem.* **1962**, *34*, 1502.
4. Taguchi, N. *Jap. Patent* 45-382, 1962.
5. Faglia, G.; Nelli, P.; Sberveglieri, G. *Sensor and Actuators B* **1994**, *18-19*, 497.
6. Saji, K. *et al. Proc. Int. Meet. on Chemical Sensors*; Fukuoka: Japan, 1983; p 171.
7. Levy, M. *et al. J. Physique. Coll.* **1991**, *6*(41), 329.
8. Wang, Y.; Wang, S.; Zhao, Y.; Zhu, B.; Kong, F.; Wang, D.; Wu, S.; Huang, W.; Zhang, S. *Sensors and Actuators B* **2007**, *125*, 79.
9. Zhan, Z.; Lu, J.; Song, W.; Jiang, D.; Xu, J. *Materials Research Bulletin* **2007**, *42*, 228.
10. Shaver, P. *Appl. Phys. Lett.* **1967**, *11*, 255.
11. Nishio, K.; Sei, T.; Tsuchiya, T. *J. Ceram. Soc. Jpn.* **1999**, *107*, 199.
12. (a) Klejnot, O. J. *Inorg. Chem.* **1965**, *4*, 1668. (b) Hocker, H.; Jones, F. R. *Macromol. Chem.* **1972**, *161*, 251.
13. Min, B. K.; Oh, S. D. *Kor. J. Ceram.* **1999**, *5*(2), 125.
14. Lim, C. H.; Oh, S. J. *Sensors and Actuators B* **1996**, *30*, 223.
15. Yoo, D. J.; Tamaki, J.; Miura, N.; Yamajoe, N.; Park, S. J. *Korean Journal of Materials Research* **1996**, *6*(7), 716.
16. Kawahara, A.; Katsuki, H.; Egashira, M. *Sensors and Actuators B* **1998**, *49*, 273.
17. Khadayate, R. S.; Sali, J. V.; Patil, P. P. *Talanta* **2007**, *72*, 1077.
18. Dean, J. A. *Lange's Handbook of Chemistry*, 13th ed.; McGraw Hill: New York, U.S.A. 1985; p 10.
19. Xu, C.; Kurokawa, J.; Miura, N.; Yamazoe, N. *J. Mater. Sci.* **1992**, *27*, 963.
20. Meng, D.; Yamajaki, Y.; Shen Y.; Liu Z.; Kikuta T. *Appl. Surf. Sci*. **2009**, *256*, 1050.
21. Matsuyama, N.; Okazaki, S.; Nakagawa, H.; Fukuda, K. *Thin Solid Films* **2009**, *517*, 4650.
22. Tutov, E. A. *Semiconductors* **2008**, *42*, 1561.
23. Khatko, V.; Vallejos, S.; Calderer, J.; Gracia, I.; Cane, C.; Llobet, E.; Correig, X. *Sens. Actuators B: Chem*. **2009**, *140*, 356.
24. Srivastava, V.; Jain, K. *Sens. Actuators B: Chem*. **2008**, *133*, 46.
25. Wu, R.-J.; Chang, W.-C.; Tsai, K.-M.; Wu, J.-G. *Sens. Actuators B: Chem*. **2009**, *138*, 35.
26. Jakubik, W. P. *Thin Solid Films* **2009**, *517*, 6188.
27. Solntsev, V. S.; Gorvanyuk, T. I.; Litovchenko, V. G.; Evtukh, A. A. *Thin Solid Films* **2009**, *517*, 6202.